



This open access document is published as a preprint in the Beilstein Archives with doi: 10.3762/bxiv.2020.67.v1 and is considered to be an early communication for feedback before peer review. Before citing this document, please check if a final, peer-reviewed version has been published in the Beilstein Journal of Nanotechnology.

This document is not formatted, has not undergone copyediting or typesetting, and may contain errors, unsubstantiated scientific claims or preliminary data.

Preprint Title Molecular dynamics modeling of formation processes parameters influence on a superconducting spin valve structure and morphology

Authors Alexander Vakhrushev, Alexey Fedotov, Vladimir Boian, Roman Morari and Anatolie Sidorenko

Publication Date 02 Jun 2020

Article Type Full Research Paper

ORCID® IDs Alexander Vakhrushev - <https://orcid.org/0000-0001-7901-8745>; Alexey Fedotov - <https://orcid.org/0000-0002-0463-3089>; Vladimir Boian - <https://orcid.org/0000-0001-5708-4098>; Anatolie Sidorenko - <https://orcid.org/0000-0001-7433-4140>

License and Terms: This document is copyright 2020 the Author(s); licensee Beilstein-Institut.

This is an open access publication under the terms of the Creative Commons Attribution License (<http://creativecommons.org/licenses/by/4.0>). Please note that the reuse, redistribution and reproduction in particular requires that the author(s) and source are credited.

The license is subject to the Beilstein Archives terms and conditions: <https://www.beilstein-archives.org/xiv/terms>.

The definitive version of this work can be found at: doi: <https://doi.org/10.3762/bxiv.2020.67.v1>

Molecular dynamics modeling of formation processes parameters influence on a superconducting spin valve structure and morphology

Vakhrushev Alexander*^{1,2,4}, Fedotov Alexey^{1,2,4}, Boian Vladimir^{3,4}, Morari Roman^{4,5} and Sidorenko Anatolie^{3,4}

Address: ¹ Department of Modeling and Synthesis of Technological Structures, Institute of Mechanics, Udmurt Federal Research Center, Ural Division, Russian Academy of Sciences, Baramzinoy 34, Izhevsk 426067, Russia,

²Department of Nanotechnology and Microsystems, Kalashnikov Izhevsk State Technical University, Studencheskaya 7, Izhevsk 426069, Russia,

³ Ghitu Institute of Electronic Engineering and Nanotechnologies, Academiei str., 3/3, MD-2028, Chisinau, Republic of Moldova,

⁴Orel State University named after I.S. Turgenev, Komsomolskaya str. 95, 302026, Orel, Russia,

⁵Laboratory of Topological Quantum Phenomena in Superconducting Systems (TQPSS), MIPT, Institutskiy per. 9, 141701, Dolgoprudny, Russia

Email: Vakhrushev Alexander email Vakhrushev-a@yandex.ru

* Corresponding author

Abstract

The work is devoted to the study of the processes of formation and analysis of the parameters of a functional nanostructure — a superconducting spin valve, which is a multilayer structure consisting of ferromagnetic cobalt nanolayers separated by niobium superconductor nanolayers. The aim of the work was to study the influence of the main parameters of the technological regimes of the formation of these nanosystems: temperature, concentration and spatial distribution of deposited atoms over the surface of the nanosystem on the atomic structure and morphology of the nanosystem. The studies were carried out by the molecular dynamics method using the many-particle potential of the modified immersed atom method. The temperature in the calculation process was controlled using the Nose-Hoover thermostat. The simulation of the formation of atomic nanolayers by the method of alternating directional deposition of layers of different compositions under high vacuum and stationary temperature conditions is performed. As a result of the studies, the structure and thickness of the formed nanolayers and the distribution of elements in the area of their interface were studied. It is shown that alternating layers of the formed layered nanosystem and their interfaces have a significantly different atomic structure depending on the main parameters of the technological regimes of the formation of layered nanosystems.

Keywords

spin valve; mathematical modeling; molecular dynamics; modified embedded-atom method; hybrid nanostructure; vacuum deposition

Introduction

Multilayer hybrid nanostructures "superconductor-ferromagnet" are a new type of elements of quantum electronics - spintronics based on electron spin transport. Unlike conventional electronics, spintronics uses not only charge transfer, but also the electron spin in solids, which serves to solve the problem of transporting and recording information [1-7]. Based on the basic non-dissipative elements of spintronics, it is possible to create new devices of superconducting nanoelectronics, consuming a minimum of energy and having high speed [8-14].

Practice shows that the creation of multilayer superconductor-ferromagnet nanostructures with the required properties is a very complex process, therefore, as a rule, it is not possible to create an "ideal" nanosystem. Fig. 1 and Fig. 2 show real multilayer nanosystems formed from various materials [9]. It can be seen from the figures that the structure of real nanosystems is far from ideal. In particular, it can be noted that the surface separating the various nanolayers of the system is not perfectly flat. The surface has noticeable irregularities that are directed into the contacting layers. The figures also show that there is a mutual penetration of atoms of one contacting layer into another. Therefore, the layer interface has a certain (non-zero) thickness.

It should be noted that the atomic structure of each layer does not form an ideal whole nanocrystal, but a system is formed that combines nanocrystals.

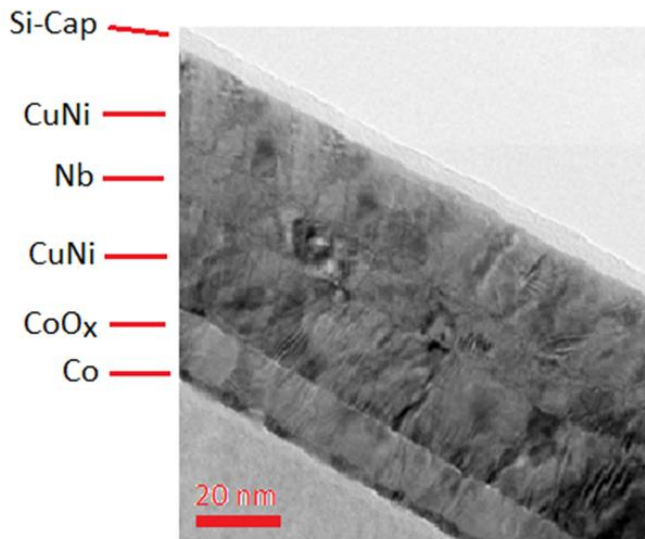


Figure 1: TEM picture of a layered nanostructure Nb, CuNi, CuOx and Co

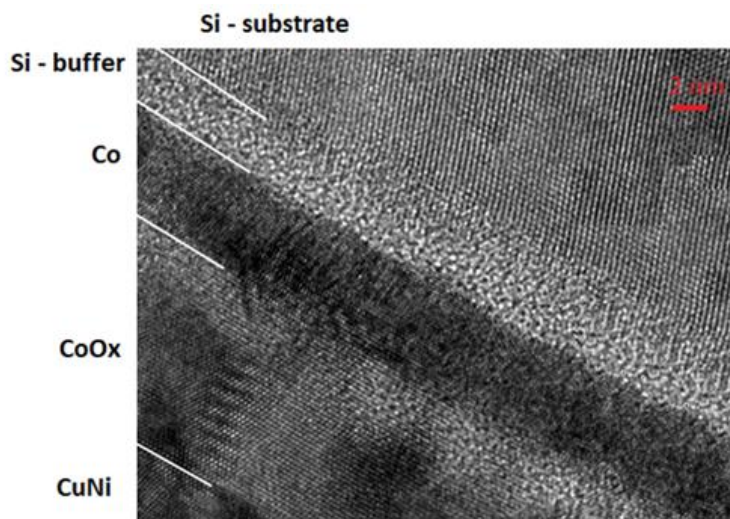


Figure 2: TEM picture of a layered nanostructure Co, CuOx and CuNi

To minimize these defects and imperfections of layered nanosystems, the implementation of optimal technological processes is required. This requires basic research for a deep understanding of the physical and chemical processes taking place at different structural levels of the materials used. In addition, the development of manufacturing technology for a fundamentally new device for superconducting

spintronics requires a long amount of time for equipment and specialists, a large number of experiments aimed at optimizing the process.

Thus, due to the laboriousness of vacuum technologies for the formation of superconductor-ferromagnet systems and the high cost and duration of experimental methods for studying the physics and chemical properties of these nanosystems, it becomes very important to develop new integrated methods that combine theoretical modeling and experimental methods for analyzing the formation processes and properties of this class functional nanomaterials and nanostructures. In this case, computer simulation can significantly reduce the number of technological steps and the required number of technology adjustments to obtain the required multilayer nanostructure.

It should be noted that mathematical modeling is widely used in the design and analysis of the properties of various nanosystems [15-17], however, in relation to the considered class of multilayer nanosystems for spintronics, the number of works is very limited. Basically, the modeling of the physical properties of ideal layered nanosystems for spintronics was carried out, in which the real structure of the nanosystem was not taken into account.

The aim of this work, as the development of previous studies of the authors on the modeling of various nanosystems [18-20], including for spintronics [21-22], was to study the influence of the main parameters of technological modes of the formation of layered nanosystems for spintronics: temperature, concentration and spatial distribution of deposited atoms over the surface of the nanosystem - on their structure and morphology.

2. Mathematical Model and Theoretical Foundations

The formation processes and the structure of multilayer systems for spintronics were studied by the molecular dynamics method [23,24]. Molecular dynamics describes the motion of each atom of a nanosystem at a certain point in time, therefore it is possible to reproduce the detailed evolution of nanoelements and their properties.

The basis of the method is the equations of motion of all atoms, supplemented by the initial conditions in the form of coordinates and velocities of atoms:

$$m_i \frac{d^2 \mathbf{r}}{dt^2} = - \frac{\nabla U(\mathbf{r})}{\|\mathbf{r}_i\|} + \mathbf{F}_{ex}, \quad \mathbf{r}_i(t_0) = \mathbf{r}_{i0}, \quad \frac{d\mathbf{r}_i(t_0)}{dt} = \mathbf{V}_{i0}, \quad i = 1, K, N, \quad (1)$$

where N – is the number of atoms that formed nanosystem.

m_i – is the mass of the i -th atom; $\mathbf{r}_{i0}, \mathbf{r}_i(t)$ – are the initial and current radius vector of the i -th atom, respectively; $U(\mathbf{r})$ - is the system potential, which depends on the relative position of all atoms; $\mathbf{V}_{i0}, \mathbf{V}_i(t)$ – are the initial and current speed of the i -th atom, respectively; $\mathbf{r}(t) = \{\mathbf{r}_1(t), \mathbf{r}_2(t), \dots, \mathbf{r}_K(t)\}$ – shows the dependence of the location of all the atoms system; \mathbf{F}_{ex} – is the external force, reflects the interaction of the nanosystem with the external environment, including responsible for adjusting the energy to maintain a constant temperature.

The molecular dynamics method is based on the concept of potential $U(\mathbf{r})$, which is responsible for the nature and magnitude of the interactions of atoms of a nanosystem.

The type of potential may be different, but recently due to its accuracy and adequacy, many-particle force fields have gained great popularity. In this work, we used the potential of the modified embedded atom method - MEAM (Modified Embedded Atom Method). The modified immersed atom method is based on the

density functional theory - DFT (Density Functional Theory). In this method, the resulting potential of the nanosystem is represented as the sum of the contributions of the energies of individual atoms, and the contributions of pair and multi-element interactions are considered separately.

$$U(r) = \sum_i U_i(r) = \sum_i \left(F_i(\bar{\rho}_i) + \frac{1}{2} \sum_{j \neq i} \phi_{ij}(r_{ij}) \right), \quad i = 1, 2, \dots, N, \quad (2)$$

where $U_i(r)$ – is a potential of an individual atom, affecting the type and degree of interaction in the equations of motion (1); F_i – is atom immersion function, dependent on electron background density $\bar{\rho}_i$; $\phi_{ij}(r_{ij})$ – is a contribution of the pair potential to the total energy, which varies with distance r_{ij} .

The immersion function is corrected by the force field created by pair interactions and refines its value. This value is due to the presence of electron gas in the material and, in accordance with [23, 24], can be calculated by the formula

$$F_i(\bar{\rho}_i) = \begin{cases} A_i E_i^0 (\bar{\rho}_i) \ln(\bar{\rho}_i), & \bar{\rho}_i \geq 0 \\ -A_i E_i^0 \bar{\rho}_i, & \bar{\rho}_i < 0 \end{cases}, \quad (3)$$

where A_i – is an empirical force field parameter; E_i^0 – is the value of sublimation energy; $\bar{\rho}_i$ – is a value of background electron density.

To calculate the background electron density at the immersion point, the following equation is used, in which all electronic orbitals of atoms of various configurations add their terms

$$\bar{\rho}_i = \frac{\rho_i^{(0)}}{\rho_i^0} G(\Gamma_i), \quad \Gamma_i = \sum_{k=1}^3 t_i^{(k)} \left(\frac{\rho_i^{(k)}}{\rho_i^{(0)}} \right)^2, \quad (4)$$

Where parameters $t_i^{(k)}$ are the weights coefficients of the model; ρ_i^0 – are the magnitude of the background electron density of the initial structure; $\rho_i^{(k)}$ – characterize the change in electron density in real conditions.

Indices $k = 1, 2, 3$ belong to different types of electronic orbitals of an atom.

Spherically symmetric one-electron s-orbital and angular electron p-, d-, f-clouds are distinguished. For each orbital, its own formula is used, in accordance with which its electronic distribution density is calculated

$$s \text{ orbital: } \rho_i^{(0)} = \sum_{i \neq j} \rho_j^{A(0)}(r_{ij}) S_{ij}, \quad (5)$$

$$p \text{ orbital: } (\rho_i^{(1)})^2 = \sum_{\alpha} \left[\sum_{i \neq j} \frac{r_{ij\alpha}}{r_{ij}} \rho_j^{A(1)}(r_{ij}) S_{ij} \right]^2, \quad (6)$$

$$d \text{ orbital: } (\rho_i^{(2)})^2 = \sum_{\alpha, \beta} \left[\sum_{i \neq j} \frac{r_{ij\alpha} r_{ij\beta}}{r_{ij}^2} \rho_j^{A(2)}(r_{ij}) S_{ij} \right]^2 - \frac{1}{3} \left[\sum_{i \neq j} \rho_j^{A(2)}(r_{ij}) S_{ij} \right]^2, \quad (7)$$

$$f \text{ orbital: } (\rho_i^{(3)})^2 = \sum_{\alpha, \beta, \gamma} \left[\sum_{i \neq j} \frac{r_{ij\alpha} r_{ij\beta} r_{ij\gamma}}{r_{ij}^3} \rho_j^{A(3)}(r_{ij}) S_{ij} \right]^2 - \frac{3}{5} \sum_{\alpha} \left[\sum_{i \neq j} \frac{r_{ij\alpha}}{r_{ij}} \rho_j^{A(3)}(r_{ij}) S_{ij} \right]^2, \quad (8)$$

where $\rho^{A(h)}$ – are radial functions; S_{ij} – is potential shielding function; $r_{ij\alpha}$ – is component α from the distance vector between atoms $\alpha, \beta, \gamma = x, y, z$.

The functional $G(\Gamma)$ in equation (4) can be defined in various ways. One of the most popular formulations is written as a dependency.

$$G(\Gamma) = \begin{cases} \sqrt{1+\Gamma}, & \Gamma \geq -1 \\ -\sqrt{|1+\Gamma|}, & \Gamma < -1 \end{cases}. \quad (9)$$

The weight coefficients of the modified immersed atom method from (4) also have an additive relationship with single-electron radial functions

$$t_i^{(k)} = \frac{\sum_{i \neq j} t_{0,j}^{(k)} \rho_j^{A(0)} S_{ij}}{\sum_{i \neq j} (t_{0,j}^{(k)})^2 \rho_j^{A(0)} S_{ij}}, \quad (10)$$

where $t_{0,j}^{(k)}$ – are empirical parameters that depend on the chemical type of the element.

Distance energy smoothing in MEAM is achieved by introducing a shielding function. Using the screening function, the attenuation of the potential occurs gradually, which allows one to provide a more physically accurate description of the properties of nanomaterials and reduce computational costs during simulation

$$S_{ij} = f_c \left(\frac{r_c - r_{ij}}{\Delta r} \right) \prod_{k \neq i, j} f_c \left(\frac{C_{ikj} - C_{\min, ikj}}{C_{\max, ikj} - C_{\min, ikj}} \right), \quad C_{ikj} = 1 + 2 \frac{r_{ij}^2 r_{ik}^2 + r_{ij}^2 r_{jk}^2 - r_{ij}^4}{r_{ij}^4 - (r_{ik}^2 - r_{jk}^2)^2}, \quad (11)$$

$$f_c(x) = \begin{cases} 1, & x \geq 1 \\ \left[1 - (1-x)^4 \right]^2, & 0 < x < 1, \\ 0, & x \leq 0 \end{cases} \quad (12)$$

where C_{\min}, C_{\max} – the parameters of the mutual influence of atoms, depending on their chemical types, are set for each triple of atoms with numbers i, j, k ; r_c – is the distance at which the force field is cut off; - a parameter exceeding the cutoff distance is used to smooth the potential.

3. Problem Statement and Software

The influence of the formation processes parameters of the spin system hybrid structures “superconductor-ferromagnet” is studied for a multilayer nanosystem based on cobalt and niobium. This system is a functional material demonstrated a giant spin-valve effect, theoretically and experimentally investigated in [25–27]. In these works the authors proposed a new design and performed the calculation of a spin valve consisting of superconducting plates and an artificial magnetic metamaterial placed between them, formed by periodically alternating thin and thick nanolayers of a ferromagnetic metal. The thickness of the layers affects the magnetic

exchange interaction between ferromagnet layers, that gives the possibility of design of artificial magnetic metamaterials with tunable properties .

The choice of niobium and cobalt as the metals forming nanolayers is dictated by the wide potential of using these elements in spintronics. At the moment, not only research were carried out on spintronic devices involving these metals [28, 29], but also new patents are being issued [30-32].

The general scheme of the investigated nanosystem is presented in Figure 3.

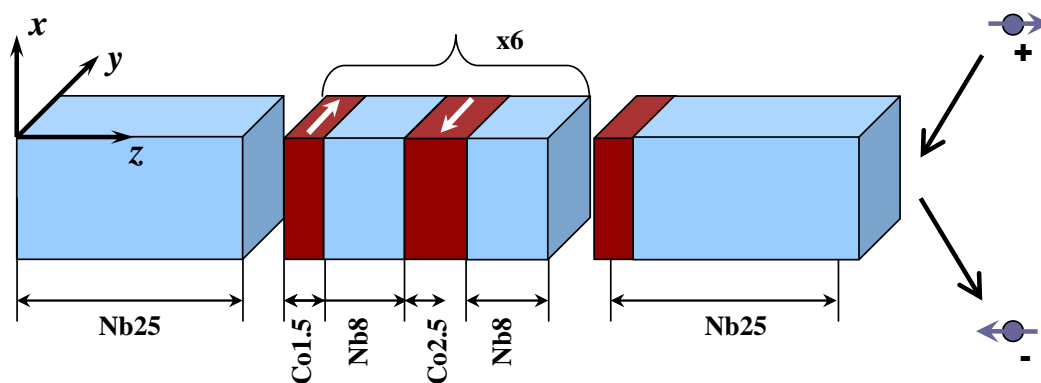


Figure 3: Sketch of a Nb/Co spin valve nanosystem

The numbers in figure 3 next to the elements in the layers presents their thickness in nanometers. Sample production is carried out by the method of magnetron deposition of materials in vacuum. In general, a nanosystem contains about 20 layers.

Nevertheless, the processes of formation are similar to each other. Therefore, in this work, we consider the deposition of only the first four layers of cobalt and niobium.

The general statement of the problem of modeling the multilayer nanosystem formation processes is presented in Figure 4.

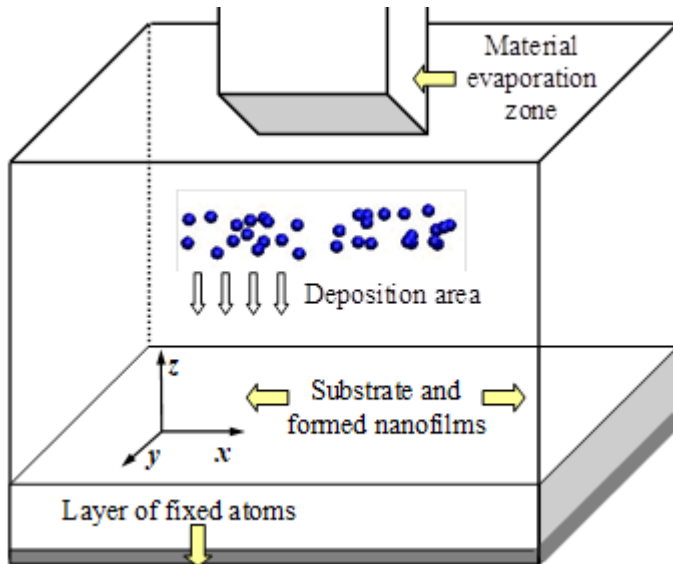


Figure 4: Scheme of modeling processes of the multilayer nanosystem

formation

The first layer of material formed by niobium atoms is the substrate and the basis for the vacuum deposition of subsequent nanofilms. The substrate is placed in the lower region of the computational cell; its extreme layer is fixed to prevent chaotic movement of the sample during the simulation. In horizontal directions, periodic boundary conditions are imposed on the computational cell, which reduce the computational cost. In the upper region, boundary reflection conditions are present so that the deposited atoms do not leave the modeling system. The deposition process is simulated by the appearance of atoms in the evaporation zone above the substrate. In this case, the deposited atoms gained speed towards the substrate. The layers are sprayed in stages. During the formation of all layers, the magnetic field in the nanosystem was absent.

The upper boundary of the computational cell was shifted during the transition to the deposition of the next nanolayer by the value of its thickness. Thus, the deposition region above the substrate turned out to be approximately the same for each layer of the nanosystem. The regulatory parameters of the process, affecting the properties of the resulting nanomaterial, were: the deposition rate, controlled through the number

of deposited atoms per unit time; substrate temperature; spraying flux density, which was determined by the area of the evaporation zone.

As the computational module of the program for theoretical research, the LAMMPS (Large-scale Atomic / Molecular Massively Parallel Simulator) computing complex was used [33]. This software and tool package is freely distributed, contains the ability to perform parallel computing and supports multilevel mathematical models, including molecular dynamics. Results analysis algorithms were described in TCL and C ++. Based on LAMMPS, scripts and algorithms were developed and implemented for a detailed study of the structure of superconductor-ferromagnet materials and the determination of its spatial profile. The results were visualized using the VMD (Visual Molecular Dynamics) [34] and OVITO (Open Visualization Tool) [35] software packages, which not only provide images of the atomic and molecular structures of nano-objects, but also construct spatial profiles and distributions by the target parameter, e.g. height or coordination number.

4. Results and Discussion

A series of numerical experiments on modeling the processes of formation of the multilayer hybrid structure based on cobalt and niobium were performed. Variable elements in the studies were the technological parameters of the fabrication of the material, including the temperature of the substrate, the intensity and area of the deposition flow. The influence of technological modes was evaluated in comparison with the basic version of the formation of a nanosystem.

As a basic variant, growth processes were considered at normal (300 K) temperature, and deposition was carried out by a uniform flow over the entire surface

of the substrate. The temperature in the nanosystem was controlled using a Nose-Hoover thermostat. The thermostat maintained the temperature of the substrate. The deposited atoms had a directed velocity; therefore, they were not involved in the direct correction of the thermostat. The formation of a multilayer system was carried out in several stages; each layer was deposited by sequential deposition of one of the metals, niobium or cobalt.

At the first stage, cobalt was deposited on a substrate formed by niobium atoms. The substrate had a crystalline structure with a height of 3.7 nm and a width of 13.2 nm in horizontal directions. For the mark of zero height, from which the layers of the deposited material began to form, the substrate surface was chosen. The number of niobium atoms in the substrate was 33600.

To match the simulation results and experimental data, and the formation of nanolayers of the required thickness, 18,000 cobalt atoms were deposited on the substrate in the first stage, 70,000 niobium atoms were deposited in the second, and 30,000 cobalt atoms were deposited in the third stage. As a result, three nanofilms with a thickness of 1.5 nm, 8.0 nm and 2.5 nm were formed. The duration of all three stages of deposition of the layers for the basic version of sample preparation under normal conditions was chosen in accordance with their thickness and amounted to 0.2 ns, 0.6 ns, and 0.4 ns. The image of a multilayer nanosystem formed as a result of mathematical modeling is presented in Figure 5.

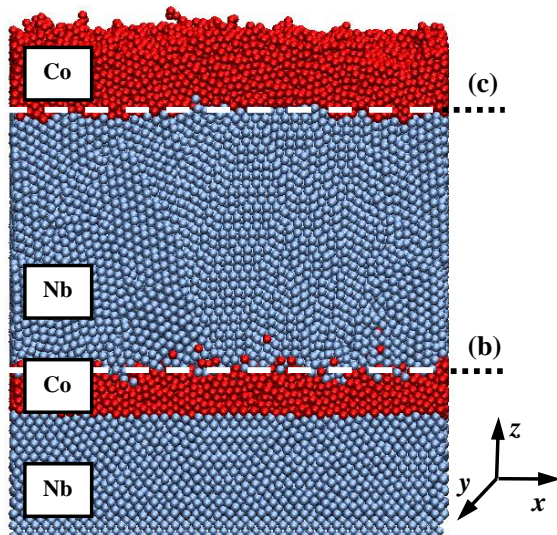


Figure 5: Multilayer nanosystem niobium and cobalt.

Substrate temperature is fixed as 300 K.

The image in Figure 5 demonstrates well the picture of the formation processes of the layered nanosystem of niobium and cobalt and the structure of the layers. The structure of the layers formed by niobium atoms is close to crystalline. In this case, groups of atoms are combined into domains with different spatial orientations. Cobalt nanofilms have an amorphous structure. The blurring of the contact area between the layers and a less even surface profile compared to niobium are noticeable.

A quantitative characteristic of the spatial structure of the material can be obtained by calculating the coordination number. The coordination number in crystallography reflects the number of nearby equally distant atoms of the same type in the crystal lattice. The number of nearest neighbors determines the packing density of the material. For different types of crystal lattices, the coordination number will be different. The cubic volume-centered lattice (characteristic of niobium) has a coordination number equal to 8, the hexagonal close-packed lattice (corresponds to cobalt) - 12. For the formed nanosystem, the change in the average value of the

coordination number in parallel layers was calculated, shown in Figure 6. The distribution of this parameter in space shown in Figure 7.

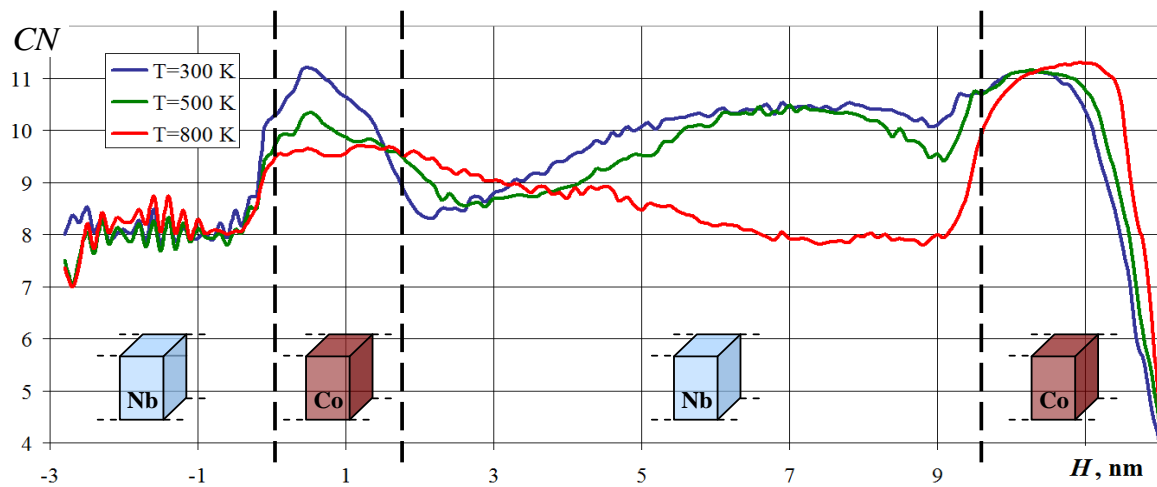


Figure 6: Change in coordination number in Nb-Co layers. Substrate temperature is 300 K.

The change in the coordination number in Fig. 6 correlates with the structure of the nanomaterial shown in Fig. 5. The niobium substrate has a parameter value close to 8, which indicates its crystalline structure. Cobalt nanofilms are characterized by an increased coordination number in the range of 10-11. This value does not reach 12, which corresponds to the ideal crystalline state of a hexagonal close-packed lattice, which indicates an amorphous-like structure of cobalt nanofilms. Variations in the coordination number within the intermediate niobium are more significant. When approaching the contact regions with cobalt, an increase in this parameter is observed. Thus, it was shown that the structure of the nanomaterial depends not only on the characteristics of the current layer, but also on the structural features of the regions adjacent to it. In addition, temperature has a definite effect on the number of nearest neighbors in a nanosystem, and therefore on its structure and properties. A significant decrease in the coordination number in the outer layers of the last

nanofilm is associated with the appearance of surface effects and boundary phenomena in that region.

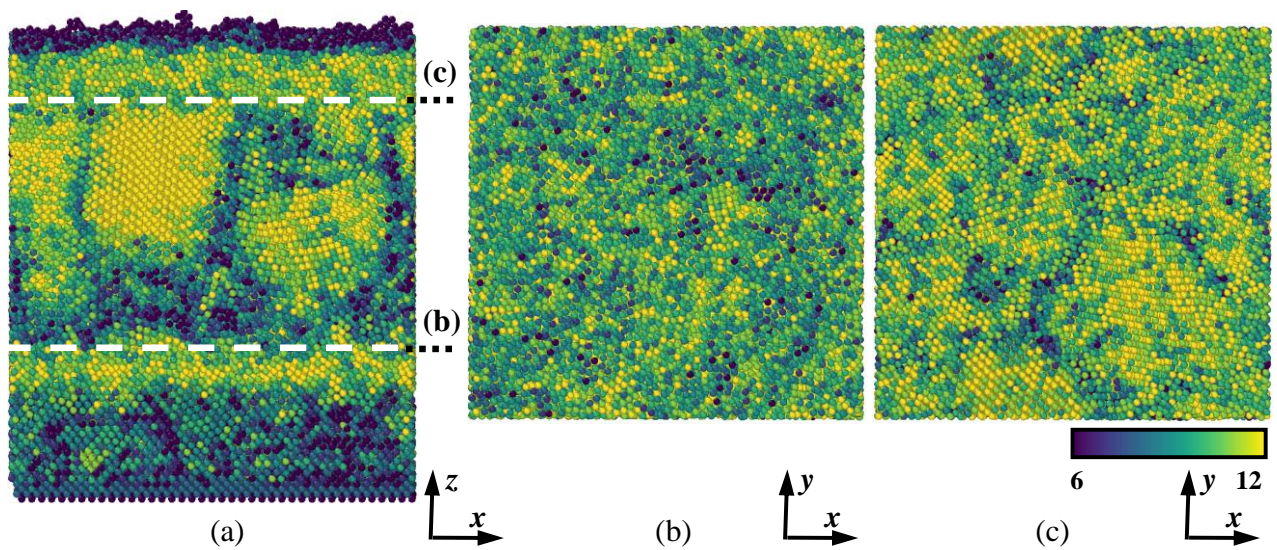


Figure 7: Spatial distribution of the coordination number in the formed multilayer Nb-Co (a) system and in its parallel sections (b) and (c). Substrate temperature 300 K.

The spatial distribution of the coordination number in the formed multilayer nanocomposite, illustrated in Figure 7, characterizes its structure in more detail. The dashed lines in Figure 7 indicate the locations of the parallel sections shown in Figure 7 (b) and Figure 7 (c). The sections correspond to the contact zones of the nanolayers and are also marked in Figure 5. The color profile of the coordination number confirms its increased value for cobalt layers. The value of the parameter in these layers is variable with a spread in a certain range of values. The niobium substrate has a lower coordination number. The structure of this region was initially crystalline and changed insignificantly during modeling and deposition. An interesting effect is observed in the intermediate niobium nanolayer, where distinct crystallization zones appeared. Crystallization zones have a higher coordination number and are characterized by a denser packing of atoms. The described regions arise in

sufficiently thick films mainly near cobalt layers. The mismatch of the crystal lattices of the starting metals causes mutual rearrangements of atoms and the transformation of the structure inside the material.

The next series of computational experiments was aimed at studying the influence of the deposition flux area and the size of the modeling region on the structure and morphology of the simulated layered nanosystem. Figure 8. shows these parameters of the nanosystem.

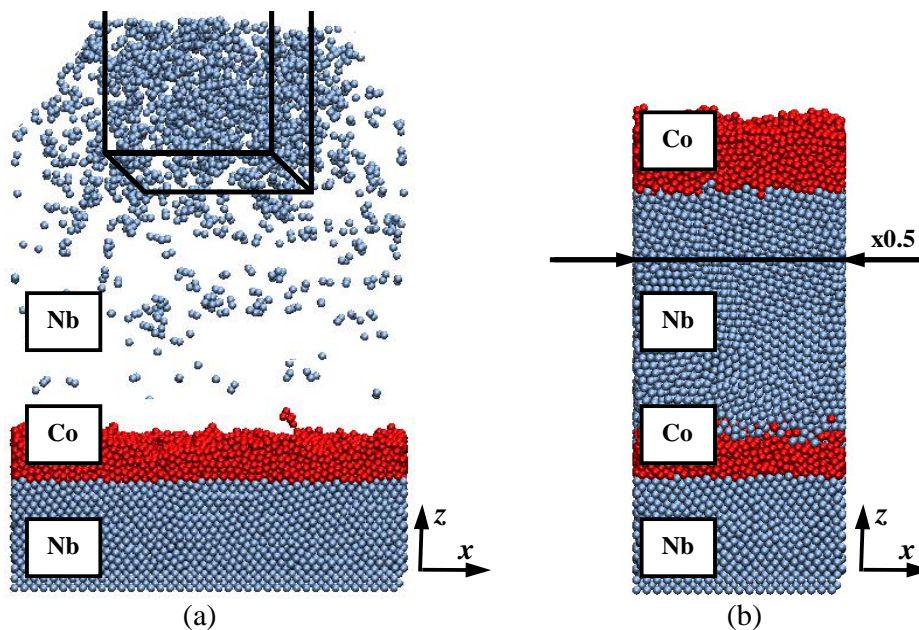


Figure 8: The area of deposition flow (a) and the size of the simulation area (b)

The change in the area of the deposition flow, illustrated in Figure 8 (a), was carried out by reducing the evaporation zone of the starting materials shown in the upper region of this figure. The spray flow area was reduced four times from the original value.

Also, modeling of nanocomposite formation processes was performed on a scale reduced by 4 times.

In this case, the number of deposited atoms in each layer was proportionally reduced so that the thickness of the formed nanofilms did not change.

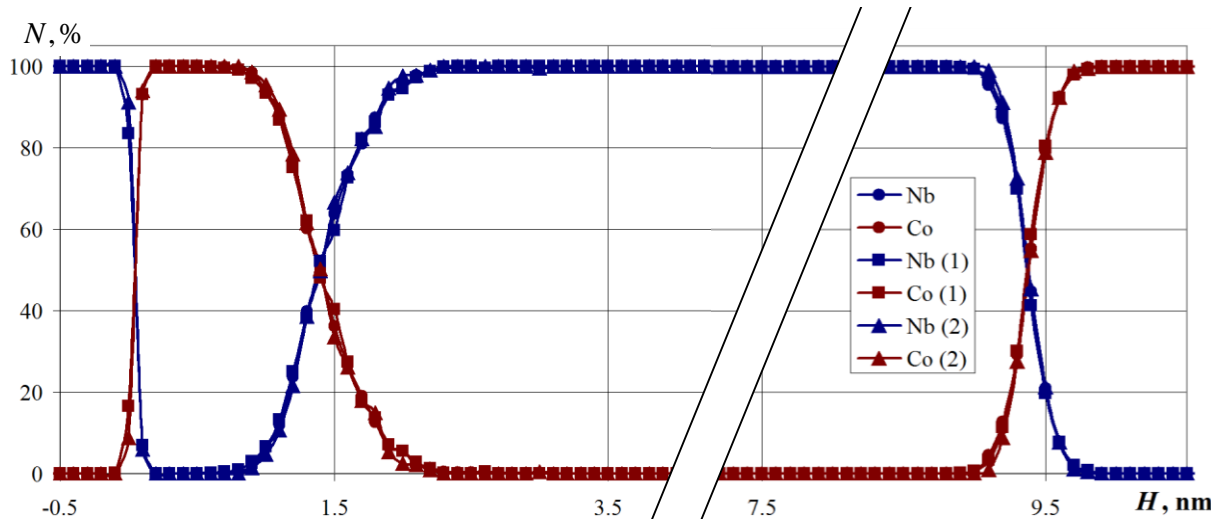


Figure 9: Relative layer-by-layer composition of the Nb-Co nanosystem for the deposition flux reduced by 4 times (1) and the modeling area reduced by 4 times (2). The temperature is 300 K.

The influence of the area of the deposition flow and the size of the modeling region on the relative layer-by-layer composition of the nanosystem are shown in Figure 9. The dependencies without an index in parentheses correspond to the basic mode of formation of the nanosystem. An analysis of the graphs shows that a change in the studied range of a decrease in the area of evaporated metals and a decrease in the calculated region do not lead to active rearrangements of atoms and a change in the composition of nanolayers. A decrease in the area of the deposition flux led only to the appearance of a zone of increased atomic density in the upper region above the substrate. Leaving the evaporation zone, the deposited atoms tend to occupy a more energetically favorable state and are scattered by an evenly distributed layer throughout the entire free volume. When the deposited atoms reach the surface of the substrate, the effect of reducing the flux is leveled.

A decrease in the transverse size of the nanosystem by 4 times also did not affect the composition of the layers of the nanosystem, which can be seen in Figure 9. The

dependences of the fractions of niobium and cobalt slightly differ from the basic version of the formation of the nanosystem.

The next series of computational experiments was aimed at elucidating the degree of dependence of the structure of a multilayer nanosystem on the flux density of deposited atoms. This value is controlled by an increase or decrease in the number of deposited atoms per unit time introduced into the system from the evaporation zone. In the work, the variants of numerical experiments on the formation of nanofilms with a 2-fold increase and a 1.5-fold decrease in the density of the flux of deposited atoms are calculated.

The relative layered composition of the nanocomposite for the calculations is shown in Figure 10. Here, the fraction of elements in the composition during the formation of nanolayers with a deposition rate reduced by 1.5 times is shown by solid lines without markers, with increased intensity by dashed lines without markers and the base atom deposition intensity by solid lines with markers.

The dependency analysis in figure 10 shows that a decrease in the deposition rate of metals did not significantly affect the distribution of the composition within the layers of a multilayer nanosystem.

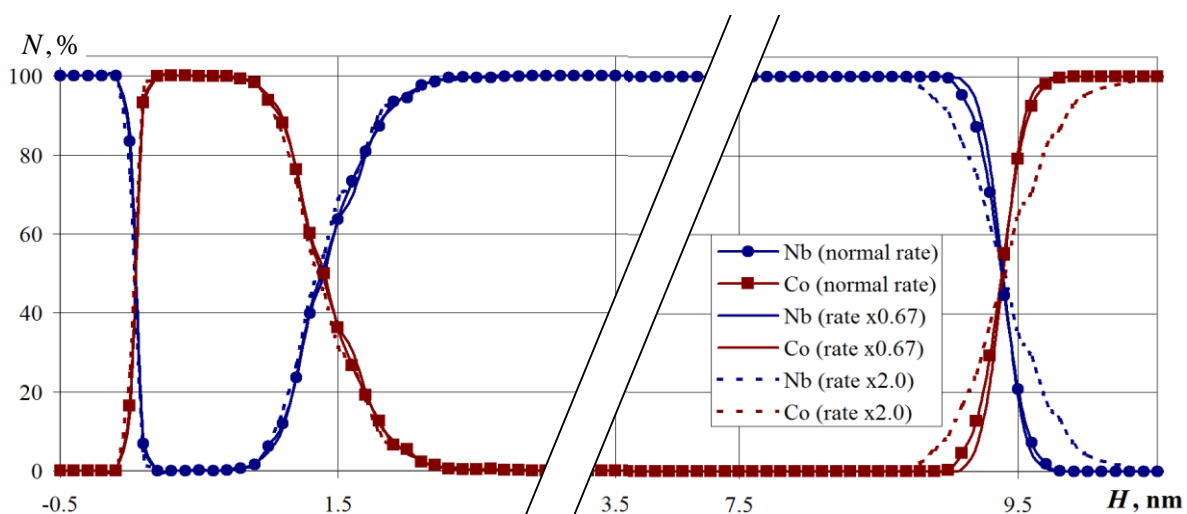


Figure 10: The relative layered composition of the nanosystem Nb-Co for different deposition rates. Temperature is 300 K

An increase in speed led to a deviation of the composition from the data obtained in the basic version of the calculation. A significant increase in the flux intensity leads to the fact that metal atoms begin to agglomerate into nanoparticles above the surface of the substrate. The structure of the resulting nanofilms directly depends on the size of the deposited clusters and does not always have time to rebuild upon direct contact with the surface. Due to the effects that arise, inhomogeneities, dislocations, and voids can occur in the material. The deviation in the constructed compositional dependences in the upper layers of the nanocomposite, where due to a more rarefied structure, additional mixing of the contact regions of the nanofilms is especially pronounced. The conducted studies indicate the presence of a certain critical deposition rate, the excess of which leads to the formation of a nanomaterial of a different structure. Since in real technological processes deposition is carried out with a sufficiently low intensity (about 1000 nm per hour), in order to obtain physically adequate research results, the deposition processes must be simulated at a speed not exceeding this critical value. On the other hand, there is no need to increase the duration of the stages of nanofilm growth, maximally approximating its real value, since, as the graphs in Fig. 10, the structure and composition in this case are similar.

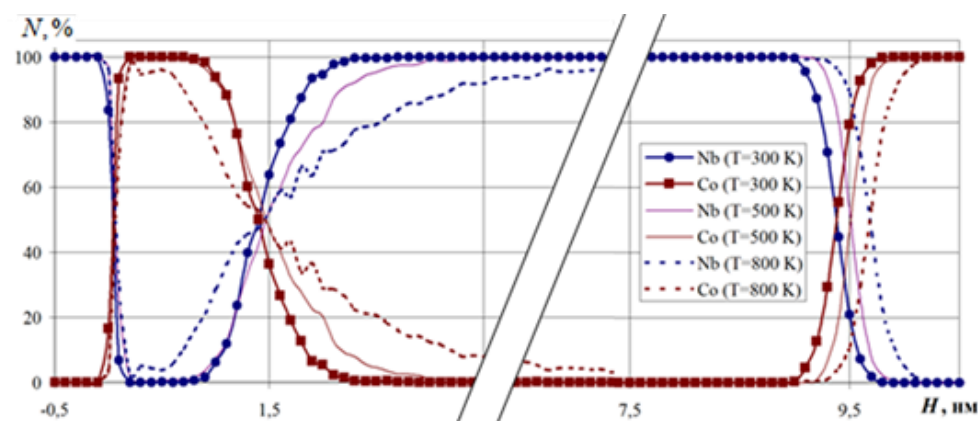


Figure 11: The percentage composition of the Nb-Co multilayer nanosystem formed at a substrate temperature of 300, 500, and 800 K, respectively

A series of computational experiments was carried out in which the formation of Nb-Co multilayer nanosystems was studied in the temperature range 300–800 K, for substrate temperatures of 300, 500, and 800 K, respectively. The simulation results are presented in Figure 11 in the form of a percentage composition graph of this nanosystem. The calculations showed that the temperature of the substrate significantly affects the formation of the structure of the nanosystem. An increase in temperature leads to an increase in the total thickness of the nanosystem (at 800 K, this value increased by 0.3 nm compared with a temperature of 300 K). The region of mutual penetration of Nb atoms into the layers of the system consisting of Co, and vice versa, is also increasing, which is clearly seen in the graphs in Figure 11. Noticeable variations in the composition of the layers of the nanosystem in the interface regions of all nanolayers are visible. The results obtained indicate a significant dependence of the processes of the formation of multilayer nanosystems, the atomic structure of the contact areas of the interface, as well as the composition and structure of the multilayer nanosystem as a whole, due to the intensification of thermal diffusion processes.

Conclusion

The paper proposes a technique and describes a mathematical model for studying technological modes and parameters in the manufacture of multilayer nanosystems. The model was tested in the study of the processes of formation of a nanosystem based on niobium and cobalt hybrid structure with the spin valve design. The influence of various technological parameters was investigated: substrate temperature, deposition flow rate and density, nanosystem sizes. Briefly, we consider the main results of the calculations.

1. An analysis of the coordination number distribution in the material showed that when multilayer nanofilms are formed under normal conditions, the layers have a different structure. The structure of the niobium substrate is close to crystalline; cobalt nanofilms are characterized by an amorphous-like structure. In the thickened niobium layer, crystallization zones are observed located in places of direct contact with the cobalt nanolayer. The mismatch of the crystal lattices of the starting metals causes mutual rearrangements of atoms and the transformation of the structure inside the nanosystem.
2. A decrease in the area of the deposition flux and the simulation region by 75% of the initial values does not lead to rearrangements of atoms and to a change in the composition of nanofilms. A decrease in the area of the deposition flux caused the appearance of a zone of increased atomic density in the upper region above the substrate.
3. The adjustment of the number of vaporized atoms per unit time and the duration of the deposition stages of nanofilms revealed the dependence of the composition of the layers and contact areas on the intensity of deposition of the starting elements. A significant increase in the intensity of the deposition flux leads to the appearance of inhomogeneities, dislocations and voids inside the formed nanosystem due to the preliminary clustering of free atoms.
4. In order to obtain physically adequate research results that correspond to real technological processes, the growth mechanisms of nanoscale films and layers must be modeled with a deposition rate not exceeding the critical value of clustering.
5. The temperature of the substrate is a leading factor affecting the formation of multilayer nanosystems, the atomic structure of the contact areas of the

interface, as well as the composition and structure of the multilayer nanosystem as a whole.

The simulation allows us to obtain detailed information on the structure and composition of multilayer nanosystems, on the mechanisms of formation of individual nanolayers and contact areas under various technological manufacturing conditions. The obtained data can be used as a supporting tool during experimental tests and for adjusting and optimizing technological processes for producing multilayer nanosystems and devices for spintronics.

Acknowledgements

The study was financially supported by the project 0427-2019-0029 Ural Branch of the Russian Academy of Sciences “Study of the laws of formation and calculation of macroparameters of nanostructures and metamaterials based on them using multilevel mathematical modeling” (chapter 2 of the article). The work was partially supported by the European Union H2020-projec “SPINTECH” under grant agreement Nr. 810144 (High-resolution TEM pictures, fig. 1 and 2) and by the Russian Science Foundation Grant (RSF) Nr. 20-62-47009 “Physical and engineering basis of computers non-von Neumann architecture based on superconducting spintronics” (The rest part of the article).

The authors are thankful to prof. Lenar Tagirov and prof. Alexander Golubov for useful discussions.

References

1. Chang, C.; Kostylev, M.; Ivanov, E. *Applied Physics Letters*. **2013**, *102*, 1-18.
doi: 10.1063/1.4800923

2. Endoh, T.; Honjo, H. *Journal of Low Power Electronics and Applications*. **2018**, 8, 1-17. doi:10.3390/jlpea8040044
3. Bell, C.; Burnell, G.; Leung, C.W.; Tarte, E.J.; Kang, D.-J.; Blamire, M.G. *Applied Physics Letters*. **2004**, 84, 1153-1155. doi: 10.1063/1.1646217
4. Deminov, R.G.; Useinov, N.Kh.; Tagirov, L.R. *Magnetic Resonance in Solids*. **2014**, 16, 14209. doi: 10.1016/j.jmmm.2014.02.033
5. Wang, Z.; Zhang, L.; Wang, M.; Wang, Z.; Zhu, D.; Zhang, Y.; Zhao, W. *IEEE Electron Device Lett.* **2018**, 39, 343-346. doi: 10.1109/LED.2018.2795039
6. Akerman, J. *Science*. **2005**, 308, 508-510. doi: 10.1126/science.1110549
7. Bai, Y.; Yang, B.; Zhang, H.; Wu, X.; Jiang, N.; Zhao, S. *Acta Materialia*. **2018**, 155, 166-174. doi: .1016/j.actamat.2018.05.069
8. Maciel, N.; Marques, E.C.; Naviner, L.A.B.; Cai, H.; Yang, J. *Microelectronics Reliability*. **2019**, 100-101, 113332. doi: 10.1016/j.microrel.2019.06.024
9. Lenk, D.; Morari, R.; Zdravkov, V.I.; Ullrich, A.; Khaydukov, Y.; Obermeier, G.; Mueller, C.; Sidorenko, A.S.; K. von Nidda, H.-A; Horn, S.; Tagirov, L.R.; Tidecks, R. *Phys. Rev. B*. **2017**, 96 , 184521/1-184521/18. oi.org/10.1103/PhysRevB.96.184521
10. Gobbi, M.; Novak, M.A.; Barco, E.D. *Journal of Applied Physics*. **2019**, 125, 240401. doi: 10.1063/1.5113900
11. Sidorenko, A. (the editor). *Functional Nanostructures and Metamaterials for Superconducting Spintronics*. Springer .**2018**. 279 pp.
12. Sidorenko, A. (the editor). *Physics, chemistry and biology of functional nanostructures II*. Beilstein Journal of Nanotechnology. **2016**. 230pp.
13. Klenov, N.; Khaydukov, Y.; Bakurskiy, S.; Morari, R.; Soloviev, I.; Boian, V.; Keller, T.; Kupriyanov, M.; Sidorenko, A.; Keimer, B. *Beilstein J. Nanotechnology*. **2019**, 10, 833–839.

14. Soloviev, I.I.; Klenov, N. V.; Bakurskiy, S. V; Kupriyanov, M.Y.; Gudkov, A.L.; Sidorenko, A.S. *Beilstein J. Nanotechnology*. **2017**, *8*, 2689–2710.
doi.org/10.3762/bjnano.8.269.
15. Steinhauser, O. M. *Computational Multiscale Modelling of Fluids and Solids. Theory and Application*. Springer-Verlag, Berlin – Heidelberg, **2008**. 427pp.
16. Weinan, E. *Principles of multiscale modeling*. Cambridge University Press, Cambridge, **2011**. 466 pp.
17. Vakhrushev, A.V. *Computational Multiscale Modeling of Multiphase Nanosystems. Theory and Applications*. Apple Academic Press, Waretown, New Jersey, **2017**. 402 pp.
18. Vakhrouchev, A. V. *Multidiscipline Modeling in Material and Structures*. **2009**, *5*, 99-118. doi: 10.1163/157361109787959895
19. Vakhrushev, A.V.; Fedotov A.Y. *Frattura Ed Integrita Strutturale*. **2019**, *49*, 370-382. doi: 10.3221/IGF-ESIS.49.37
20. Vakhrushev A.V., Fedotov A.Y., *European Physical Journal: Special Topics*. **2020**, *229*, 305-314. doi: 10.1140/epjst/e2019-900105-0
21. Vakhrushev, A.V.; Fedotov A.Yu.; Savva Yu.B.; Sidorenko A.S. *Chemical Physics and Mesoscopic*. **2019**, *21*, 362-374. doi: 10.15350/17270529.2019.3.38
22. Sidorenko A.S.; Boian V.; Savva Yu.B.; Fedotov A.Yu.; Vakhrushev, A.V. *Functional nanostructures superconductor-ferromagnet for spintronics. Proceedings of the International Symposium Nanophysics and Nanoelectronics*. **2020**, *1*, 114-115
23. Baskes, M.I. *Physical Review B* **1992**, *46*, 2727-2742. doi: 10.1103/PhysRevB.46.2727
24. Baskes, M.I.; Srinivasan, S.G.; Valone, S.M.; Hoagland, R.G. *Physical Review B*. **2007**, *75*, 094113. doi: 10.1103/PhysRevB.75.094113

25. Klenov, N.; Khaydukov, Y.; Bakurskiy, S.; Morari, R.; Soloviev, I.; Boian, V.; Keller, T.; Kupriyanov, M.; Sidorenko, A.; Keimer, B. *Beilstein J. Nanotechnology*. **2019**, *10*, 833-839. doi: 10.3762/bjnano.10.83
26. Zdravkov, V.I.; Kehrle, J.; Obermeier, G.; Lenk, D.; Krug von Nidda, H.-A.; Muller, C. Kupriyanov, M.Yu.; Sidorenko, A.S.; Horn, S.; Tidecks, R.; Tagirov, L.R. *Physical Review B*. **2013**, *87*, 144507. doi: 10.1103/PhysRevB.87.144507
27. Sidorenko, A.C. *Low Temperature Physics*. **2017**, *43*, 766–771. doi: 10.1063/1.4995623
28. Jamet, M.; Dupuis, V.; Melinon, P.; Guiraud, G.; Perez, A.; Wernsdorfer, W.; Traverse, A.; Baguenard, B. *Physical Review B* **2000**, *62*, 493-499. doi: 10.1103/PhysRevB.62.493
29. Chen, G.; Wang, Y.; Sunarso, J.; Liang, F.; Wang, H. *Energy* **2016**, *95*, 137-143. doi: 10.1016/j.energy.2015.11.061
30. Gill, H.S. *U.S. Patent No. 6665155*. 16 Dec. 2003.
31. Pinarbasi, M. *U.S. Patent No. 6353518*. 5 Mar. 2002.
32. Ju, K.; Horng, C.; Zheng, Y.; Liao, S.; Chang, J.W. *U.S. Patent No. 6995959*. 7 Feb. 2006.
33. Plimpton, S. *Journal of Computational Physics* **1995**, *117*, Pp. 1-19. doi: 10.1006/jcph.1995.1039
34. Humphrey, W.; Dalke, A.; Schulten, K. *Journal of Molecular Graphics* **1996**, *14*, 33-38. doi: 10.1016/0263-7855(96)00018-5
35. Stukowski, A. *Modelling and Simulation in Materials Science and Engineering* **2009**, *18*, 015012. doi: 10.1088/0965-0393/18/1/015012